Does diversity beget diversity in microbiomes?

Authors: Naïma Madi[1], Michiel Vos[2], Carmen Lia Murall[1],
Pierre Legendre[1] and B. Jesse Shapiro[1,3,4*]

1. Département de sciences biologiques, Université de Montréal, Canada
2. European Centre for Environment and Human Health, University of Exeter, Penryn, UK
3. Department of Microbiology and Immunology, McGill University, Canada
4. McGill Genome Centre, McGill University, Canada

*correspondence: jesse.shapiro@mcgill.ca

keywords: microbiome, evolution, ecology, Earth Microbiome Project, 16S rRNA

Abstract

Microbes are embedded in complex communities where they engage in a wide array of intra- and inter-specific interactions. The extent to which these interactions drive or impede microbiome diversity is not well understood. Historically, two contrasting hypotheses have been suggested to explain how species interactions could influence diversity. 'Ecological Controls' (EC) predicts a negative relationship, where the evolution or migration of novel types is constrained as niches become filled. In contrast, 'Diversity Begets Diversity' (DBD) predicts a positive relationship, with existing diversity promoting the accumulation of further diversity via niche construction and other interactions. Using high-throughput amplicon sequencing data from the Earth Microbiome Project, we provide evidence that DBD is strongest in low-diversity biomes, but weaker in more diverse biomes, consistent with biotic interactions initially favoring the accumulation of diversity (as predicted by DBD). However, as niches become increasingly filled, diversity hits a plateau (as predicted by EC).

Impact statement:

Microbiome diversity favors further diversity in a positive feedback that is strongest in lower-diversity biomes (*e.g.* guts) but which plateaus as niches are increasingly filled in higher-diversity biomes (*e.g.* soils).

Introduction

The majority of the genetic diversity on Earth is encoded by microbes (Hug et al., 2016; Lapierre & Gogarten, 2009; Sunagawa et al., 2015) and the functioning of all Earth's ecosystems is reliant on diverse microbial communities (Falkowski et al., 2008). High-throughput 16S rRNA gene amplicon sequencing studies continue to yield unprecedented insight into the taxonomic richness of microbiomes (e.g. (Louca et al., 2019; Sogin et al., 2006)), and abiotic drivers of community composition (e.g. pH; Lauber et al., 2009; Power et al., 2018) are increasingly characterized. Although it is known that biotic (microbe-microbe) interactions can also be important in determining community composition (Needham & Fuhrman, 2016), comparatively little is known about how such interactions, either positive (e.g. cross-feeding; Seth & Taga, 2014) or negative (e.g. toxin-mediated interference competition; Czárán et al., 2002; Hibbing et al., 2010), shape microbiome diversity as a whole.

The dearth of studies exploring how microbial interactions could influence diversity stands in marked contrast to a long research tradition on biotic controls of plant and animal diversity (Elton, 1946; Gause, 2003). In an early study of 49 animal (vertebrate and invertebrate) community samples, Elton plotted the number of species versus the number of genera and observed a ~1:1 ratio in each individual sample, but a ~4:1 ratio when all samples were pooled (Elton, 1946). He took this observation as evidence for competitive exclusion preventing related species, more likely to overlap in niche space, to co-exist. This concept, more recently referred to as niche filling or Ecological Controls (EC) (Schluter & Pennell, 2017), predicts speciation (or, more generally, diversification) rates to decrease with increasing standing species diversity

because less niche space is available (Rabosky & Hurlbert, 2015). In contrast, the Diversity Begets Diversity (DBD) model predicts that when species interactions create novel niches, standing biodiversity favors further diversification (Calcagno et al., 2017; Whittaker, 1972). For example, niche construction (i.e. the physical, chemical or biological alteration of the environment) could influence the evolution of the species constructing the niche, as well as that of co-occurring species (Laland et al., 1999; San Roman & Wagner, 2018). An alternative to either EC or DBD is The Neutral Theory of Biodiversity and Biogeography, in which all species are functionally equivalent and communities assemble via random sampling (Hubbell, 2001). Neutral Theory serves as a null hypothesis of community assembly in macrobes (Azaele et al., 2016; N. J. Gotelli & McGill, 2006), and more recently in microbiome research (Harris et al., 2017; Li & Ma, 2016).

Empirical evidence for the action of EC vs. DBD in natural plant and animal communities has been mixed (Calcagno et al., 2017; Emerson & Kolm, 2005; Palmer & Maurer, 1997; Price et al., 2014; Rabosky et al., 2018). Laboratory evolution experiments tracking the diversification of a focal bacterial lineage in communities of varying complexity have also yielded contradictory results, with support for EC, DBD, or intermediate scenarios (Brockhurst et al., 2007; Meyer & Kassen, 2007). For example, diversification of a focal *Pseudomonas* clone was favored by increasing community diversity in the range of 0-20 other strains or species within the same genus (Calcagno et al., 2017; Jousset et al., 2016) but diversification was inhibited in highly diverse communities (*e.g.* hundreds or thousands of species in compost; (Gómez & Buckling,

83 2013)). These experiments are consistent with interspecific competition initially driving
84 (Bailey et al., 2013), but eventually inhibiting diversification as niches are filled.
85 Most laboratory experiments are restricted to relatively short evolutionary time
86 scales and include only a small number of taxa; it is therefore unclear if they can be
87 generalized to natural communities consisting of many more taxa evolving and
88 assembling over much longer periods, spanning more environmental change, greater
89 evolutionary diversification, and frequent migration events. Although the absence of a
90 substantial prokaryotic fossil record hinders deconvoluting speciation and extinction rates
91 (Louca & Pennell, 2020; Marshall, 2017), Louca et al. (Louca et al., 2018) recently
92 estimated that bacterial diversity has mostly increased over the past billion years, with
93 speciation rates slightly exceeding extinction rates. However, because many free-living
94 microbes have high migration rates ("everything is everywhere, but the environment
95 selects" (de Wit & Bouvier, 2006)), we expect that the majority of diversity present
96 within a typical microbiome sample is selected from a pool of migrants rather than
97 having evolved *in situ*. As such, here we broadly define "diversity begets diversity"
98 (DBD) to include the combined effects of community assembly from a migrant pool
99 ('ecological species sorting') and *in situ* evolutionary diversification (**Fig. 1**).
100

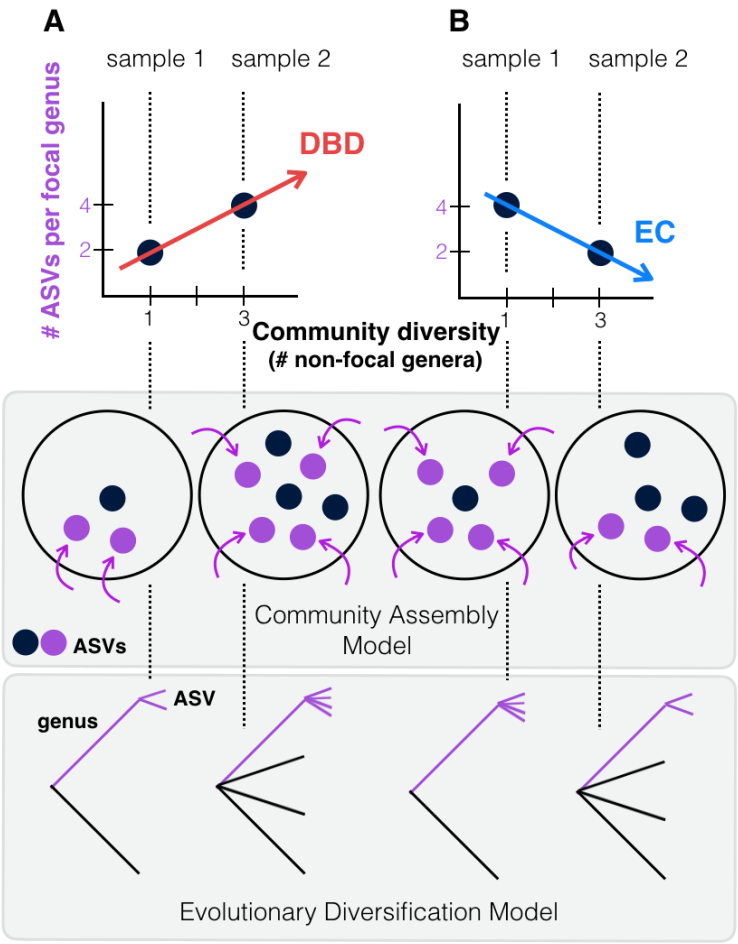

Fig. 1. Contrasting the Diversity Begets Diversity (DBD) and Ecological Controls (EC) models. (A) In this hypothetical scenario, microbiome sample 1 contains one non-focal genus, and two amplicon sequence variants (ASVs) within the focal genus (point at x=1, y=2 in the plot). Sample 2 contains three non-focal genera, and four ASVs within the focal genus (point at x=3, y=4). Tracing a line through these points yields a positive diversity slope, supporting the DBD model (red). **(B)** Alternatively, a negative slope would support the Ecological Controls (EC) model (blue line). In the middle panel, we consider a community assembly model to explain the hypothetical data of the top panel, in which standing diversity (black points) in a community selects (for or against) new types (referred to here as ASVs) which arrive via migration (purple points & arrows). In the bottom panel, we consider an evolutionary diversification model of a focal lineage (genus) into ASVs as a function of initial genus-level community diversity present at the time of diversification.

To test whether patterns of diversity in natural communities conform to EC or DBD dynamics, we used 2,000 microbiome samples from the Earth Microbiome Project (EMP), the largest available repository of biodiversity based on standardized sampling and sequencing protocols, with 16S rRNA gene amplicon sequence variants (ASVs) as the finest-grained taxonomic unit (Thompson et al., 2017). Following Elton (Elton, 1946), we use the equivalent of Species:Genus ratios, calculating a range of taxonomic diversity ratios (up to the Class:Phylum level) as proxies for diversity within a focal taxon, from shallow to deep evolutionary time. We then plot each ratio as a function of the number of non-focal taxa (Genera, Families, Orders, Classes, and Phyla, respectively) with which the focal taxon could interact. We refer to the slope of these plots as the "diversity slope", with negative slopes supporting EC and positive slopes supporting DBD (**Fig. 1**). As a null, we compare these slopes to the expectation under Neutral Theory. To avoid a trivially positive diversity slope due to variation in sequencing effort, all samples were rarefied to 5,000 observations (counts of 16S rRNA gene sequences), as diversity estimates are highly sensitive to sampling effort (Nicholas J. Gotelli & Colwell, 2001). As 16S evolves at a rate of roughly 1-2 substitutions per million years (Kuo & Ochman, 2009b), evolutionary diversification within individual EMP samples cannot be uncovered using this marker; rather our data represent mainly a record of community assembly.

Results

Quantifying the DBD-EC continuum in prokaryote communities compared to neutral null models. We used generalized linear mixed models (GLMMs) to estimate the diversity slope at each taxonomic level in the EMP data, which revealed a tendency toward positive slopes with significant variation explained by the random effects of lineage, environment, and their interaction (**Table 1, Figure 2, Figure 2 supplements 1-6, Supplementary Data file 1 Section 1**). All models reported here provide significantly better fits compared to models without the fixed effect of community diversity, and coefficients of determination (R^2) are higher with the inclusion of random effects, showing their importance (**Supplementary Data file 2**). Examples of how the diversity slope varies across lineages and environments are shown in **Figure 2** and **Figure 2 supplements 2-6**. To assess the significance of these slope estimates in light of potential sampling bias and data structure (Gotelli & Colwell, 2001; Jarvinen, 1982), we considered null models, all of which randomize the associations between ASVs within a sample, thus randomizing any true biotic interactions. Models 1 and 2 are based on draws from the zero-sum multinomial (ZSM) distribution, which arises from the standard Neutral Theory of Biodiversity (**Methods**). Model 1, in which each microbiome sample is drawn from the same ZSM distribution, produces a significantly negative diversity slope (**Figure 2 supplement 7; Table 2**). Model 2, in which each environment draws from a separate distribution, is effectively a composite of Model 1 in which different environments, each with a negative slope, are 'stacked' to yield an overall positive slope (**Figure 2 supplement 7**). However, the Model 2 slope is not significant in a GLMM

accounting for variation across environments (**Table 2, Supplementary Data file 3 Section 1.2**). In the real EMP data, most individual environments tend toward a positive slope (**Figure 2 supplement 8**). The tendency toward positive diversity slopes in the EMP is therefore not straightforwardly explained by neutral processes.

To estimate the power to detect either DBD or EC, we specifically added each of these effects to data simulated under a null model. As expected, adding DBD reversed the negative slope and rendered it positive (**Table 2; Figure 2 supplement 7, Supplementary Data file 3 Section 2.1**), suggesting reasonable power to detect DBD when truly present. In contrast, the addition of EC had little effect on the slope, suggesting low power to detect EC under some null models. Taken together, these modelling results suggest that positive diversity slopes observed in the EMP are more readily explained by DBD than by Neutral Theory, whereas negative slopes could be explained by EC, Neutral Theory, or some combination of the two.

Because taxonomic labels can be unavailable or inconsistent with phylogenetic relationships (Parks et al., 2018; Vos, 2011) we repeated the analyses using nucleotide sequence identity in the 16S rRNA gene instead of taxonomy, and again recovered generally positive diversity slopes (**Methods**). As a final sensitivity analysis, we repeated the GLMMs using unrarefied community Shannon diversity instead of richness (**Methods**) and obtained similar results, with generally positive diversity slopes that could in some cases be reversed depending on the lineage or environment (**Table 3, Supplementary Data file 1 Section 2**). The Shannon diversity metric is robust to sampling effort, suggesting that the results are not biased by undersampling in diverse biomes. Even if undersampling could bias the diversity slope downward in more diverse

samples, the effect is unlikely to be large at a rarefaction to 5,000 sequences, and only to occur at the extremes of diversity (*e.g.* very many genera and high ASV:genus ratios) and not at higher taxonomic levels (*e.g.* Class:Phylum) (**Figure 2 supplement 9**).

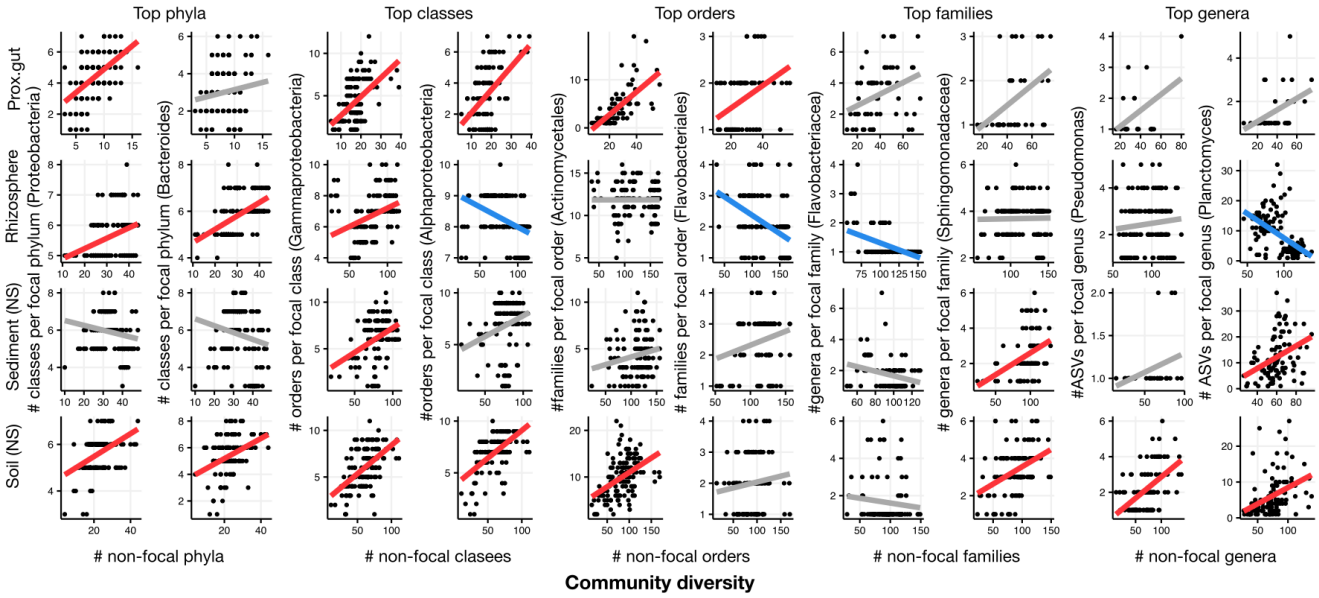

Fig. 2. Focal lineage diversity as a function of community diversity in the top two most prevalent taxa at each taxonomic level. As in **Fig. 1**, the x-axes show community diversity in units of the number of non-focal taxa (*e.g.* the number of non-Proteobacteria phyla for the left-most column), and the y-axes show the taxonomic ratio within the focal taxon (*e.g.* the number of classes within Proteobacteria). Significant positive diversity slopes are shown in red, negative in blue (linear models, $P < 0.05$, Bonferroni corrected for 17 tests), and non-significant in grey. Note that linear models are distinct from GLMMs, and are for illustrative purposes only. Four representative environments are shown (see **Figure 2 supplements 2-6** for plots in all 17 environments).

DBD reaches a plateau at high diversity. It is expected from theory and experimental studies that a positive DBD relationship should eventually reach a plateau, giving way to EC as niches become saturated (Brockhurst et al., 2007; Gómez & Buckling, 2013). This

200 expectation is borne out in our dataset, particularly in the nucleotide sequence-based
201 analyses which support quadratic or cubic relationships over linear diversity slopes
202 (**Figure 2 supplement 10**). For example, in the animal distal gut, a relatively low-
203 diversity biome, we observed a strong linear DBD relationship at most phylogenetic
204 depths; in contrast, the much more diverse soil biome clearly reaches a plateau (**Figure 2**
205 **supplement 11**).

206 To comprehensively test the hypothesis that more diverse microbiomes
207 experience weaker DBD due to saturated niche space, we used a GLMM including the
208 interaction between diversity and environment as a fixed effect. We considered this
209 model only for taxonomic ratios with significant diversity slope variation by environment
210 (**Table 1**): Family:Order, Order:Class, and Class:Phylum. Diversity slopes were
211 significantly higher in less diverse (often host-associated) biomes, suggesting that niche
212 filling leads to a plateau of DBD in more diverse biomes (**Fig. 3, Supplementary Data**
213 **file 1 Section 3**). The interaction observed in the real EMP data between community
214 diversity and biome type in shaping focal lineage diversity was not observed under a
215 neutral null (Model 2, in which each environment has its own characteristic level of
216 diversity) (**Supplementary Data file 3 Section 1.2**). The DBD plateau observed in more
217 diverse biomes is thus not readily explained by a neutral model, nor is rarefaction
218 expected to bias the diversity slope estimates, particularly at the Class:Phylum level
219 (**Figure 2 supplement 9**). This suggests that the plateau of DBD at higher levels of
220 community diversity is not an artefact of data structure or sampling effort. Finally, we
221 considered whether variation along the EC-DBD continuum could be explained by
222 differential cell density across environments, which could affect both the frequency of

223 cell-cell interactions (a biological effect) or the sampling depth (a technical artefact).
224 Although precise estimates of cell densities in all EMP biomes are not available, we
225 extracted plausible ranges for eight biomes from the literature (Kennedy & de Luna,
226 2005; Lindow & Brandl, 2003; Sender et al., 2016; Whitman et al., 1998) and annotated
227 these in **Figure 3**. It is clear from this figure that relatively high- and low-density samples
228 are found along the range of community taxonomic diversities, demonstrating that cell
229 density is unlikely to drive the trend of decreasing diversity slopes with increasing
230 community diversity.
231

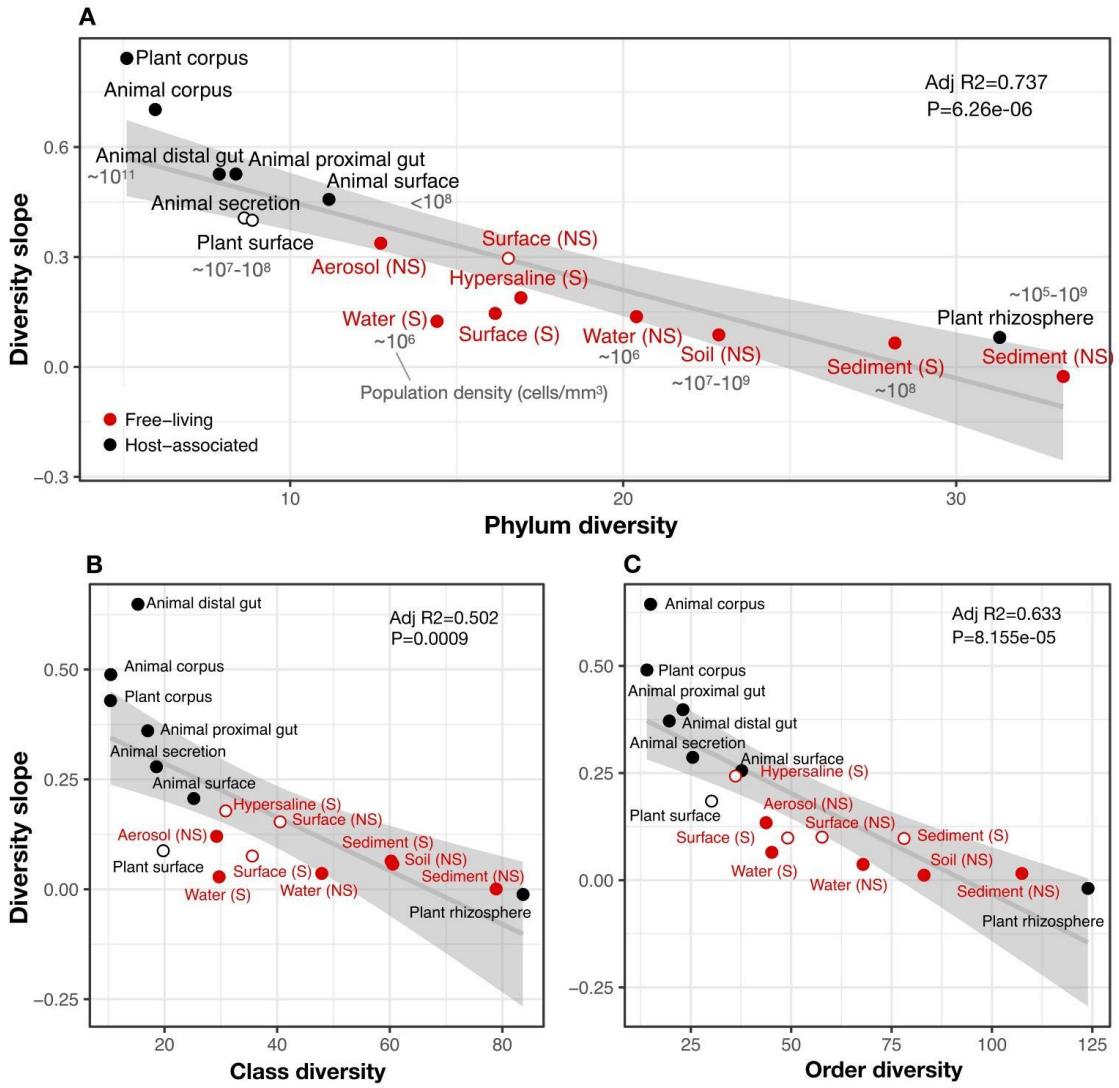

232

233 **Fig. 3. The diversity slope of focal taxa is higher in low-diversity (often host-**
234 **associated) microbiomes.** The x-axis shows the mean number of non-focal taxa: (A)
235 phyla, B) classes, and C) orders in each biome. On the y-axis, the diversity slope was
236 estimated by a GLMM predicting focal lineage diversity as a function of the interaction
237 between community diversity and environment type at the level of A) Class:Phylum, B)
238 Order:Class, and C) Family:Order ratios (**Supplementary Data file 1 Section 3**). The
239 line represents a linear regression; the shaded area depicts 95% confidence limits of the
240 fitted values. Adjusted R^2 and P-values from the linear fits are shown at the top right of
241 each panel. See **Supplementary Data file 2** for model goodness of fit. Slopes not
242 significantly different from zero are shown as empty circles. Estimates of bacterial cell

density from the literature are indicated in grey text, in units of bacteria/mm^3. For animal (skin) and plant surface, units of bacteria/mm^2 were converted to mm^3 assuming layers of bacteria 1 micron thick. For rhizosphere samples we assume a density of 1-2g/cm^3 (Kennedy & de Luna, 2005).

Abiotic drivers of diversity. Our results thus far suggest that community diversity is a major determinant of the EC-DBD continuum, and by extension that biotic interactions may override abiotic factors in determining where a community lies on the continuum. To formally test for the additional role abiotic drivers might play in generating the observed EC-DBD continuum, we analyzed two data sets in more detail.

First, we analyzed a subset of 192 EMP samples with measurements of four key abiotic factors shown to affect microbial diversity (pH, temperature, latitude, and elevation; (Delgado-Baquerizo et al., 2018; Lauber et al., 2009; Power et al., 2018; Schluter & Pennell, 2017)). We fitted a GLMM with focal lineage-specific diversity as the dependent variable, and with the number of non-focal lineages, the four abiotic factors and their interactions as predictors (fixed effects). As in the full EMP dataset (**Table 1**), focal lineage diversity was positively associated with community diversity at all taxonomic ratios in the EMP subset (**Table 4**). As expected, certain abiotic factors, alone or in combination with diversity, had significant effects on focal lineage diversity (**Table 4**). However, the effects of abiotic factors were always weaker than the effect of community diversity (**Table 4**; **Supplementary Data file 1 Section 4**).

Second, we used a global 16S sequencing dataset of 237 soil samples associated with more detailed environmental metadata (Delgado-Baquerizo et al., 2018) which we reprocessed to yield ASVs comparable to those in the EMP (**Methods**). This dataset

267 revealed weaker evidence for DBD and stronger effects of abiotic variables on diversity.
268 Community diversity generally had significant positive effects on focal-lineage diversity,
269 but the effect was weak and not detectable at all taxonomic ratios (**Table 5**). Known
270 abiotic drivers of soil bacterial diversity such as pH (Lauber et al., 2009) and latitude
271 (Delgado-Baquerizo et al., 2018) had effects of similar or stronger magnitude compared
272 to the effect of community diversity (**Table 5, Supplementary Data file 4**). The
273 relatively weak effect of DBD and strong effect of abiotic drivers on diversity in this soil
274 dataset can be explained by the fact that soils generally are highly diverse and have
275 relatively low diversity slopes (**Figure 3**).
276 We note that it remains possible that unmeasured abiotic effects could explain
277 some of the DBD effects observed in the EMP. Although only a small subset of abiotic
278 factors was considered, the generally positive diversity slopes in the EMP are not likely
279 to be driven by these factors in the abiotic environment (**Table 4**). Specifically, we
280 consider it unlikely that unmeasured abiotic factors would always act similarly, and in the
281 same direction across multiple different environments, to drive DBD. However, as
282 demonstrated in soil (**Table 5**), abiotic factors may become increasingly important in
283 highly diverse biomes with weak DBD.
284
285 **DBD is more pronounced in resident taxa than in migrant- or generalist taxa.** A
286 recent meta-analysis of 16S sequence data from a variety of biomes suggests there is an
287 important distinction between generalist lineages found in many environments, compared
288 to specialists with a more restricted distribution (Sriswasdi et al., 2017). Generalists were
289 inferred to have higher speciation rates, suggesting that the DBD-EC balance might differ

290 between generalists and specialists (Sriswasdi et al., 2017). To further investigate this
291 difference, we defined 'residents', taxa with a strong preference for a specific biome, in
292 addition to generalists without a strong biome preference in the EMP dataset. We first
293 clustered environmental samples by their genus-level community composition using
294 fuzzy *k*-means clustering (**Fig. 4a**), which identified three major clusters: 'animal-
295 associated', 'saline', and 'non-saline'. The clustering included some outliers (*e.g.* plant
296 corpus grouping with animals), but was generally consistent with known distinctions
297 between host-associated vs. free-living (Thompson et al., 2017), and saline vs. non-saline
298 communities (Auguet et al., 2010; Lozupone & Knight, 2007). Resident genera were
299 defined as those with a strong preference for a particular environment cluster (whether
300 due to dispersal limitation or narrow niche breadth) using indicator species analysis
301 (permutation test, $P<0.05$; **Fig. 4a**; **Figure 4 supplement 1**; **Supplementary Data file 5**),
302 and genera without a strong preference were considered generalists. When residents of
303 one environmental cluster were (relatively infrequently) observed in a different cluster,
304 we defined them as "migrants" in that sample. For each environment cluster, we ran a
305 GLMM with resident genus-level diversity (the number of non-focal genera) as a
306 predictor of focal-lineage diversity (the ASV:Genus ratio) for residents, generalists, or
307 migrants to that sample (**Supplementary Data file 1 Section 5**).
308 Resident community diversity had no significant effect on the diversity of
309 generalists in animal-associated, saline and non-saline clusters (GLMM, Wald test,
310 $P>0.05$), but was positively correlated with lineage-specific resident diversity (GLMM,
311 Wald test, z=7.1, P= 1.25e-12; z=3.316, P=0.0009; z=7.109, P=1.17e-12, respectively).
312 Resident community diversity significantly decreased migrant diversity in saline

313 (GLMM, z=-3.194, *P*=0.0014) and non-saline environment clusters (GLMM, z=-2.840,

314 *P*=0.0045), but had no significant effect in the animal-associated cluster (GLMM,

315 *P*>0.05) (**Fig. 4b**). These results suggest that, although generalist lineages may have

316 higher speciation rates and colonize more habitats than specialists (Sriswasdi et al.,

317 2017), they have lower diversity slopes. Migrants to the "wrong" environment experience

318 even less DBD, and are even subject to EC in two out of three environment types (**Fig.**

319 **4b**). The accumulation of diversity via successful establishment of migrants may thus be

320 limited, presumably because most niches are already occupied by residents.

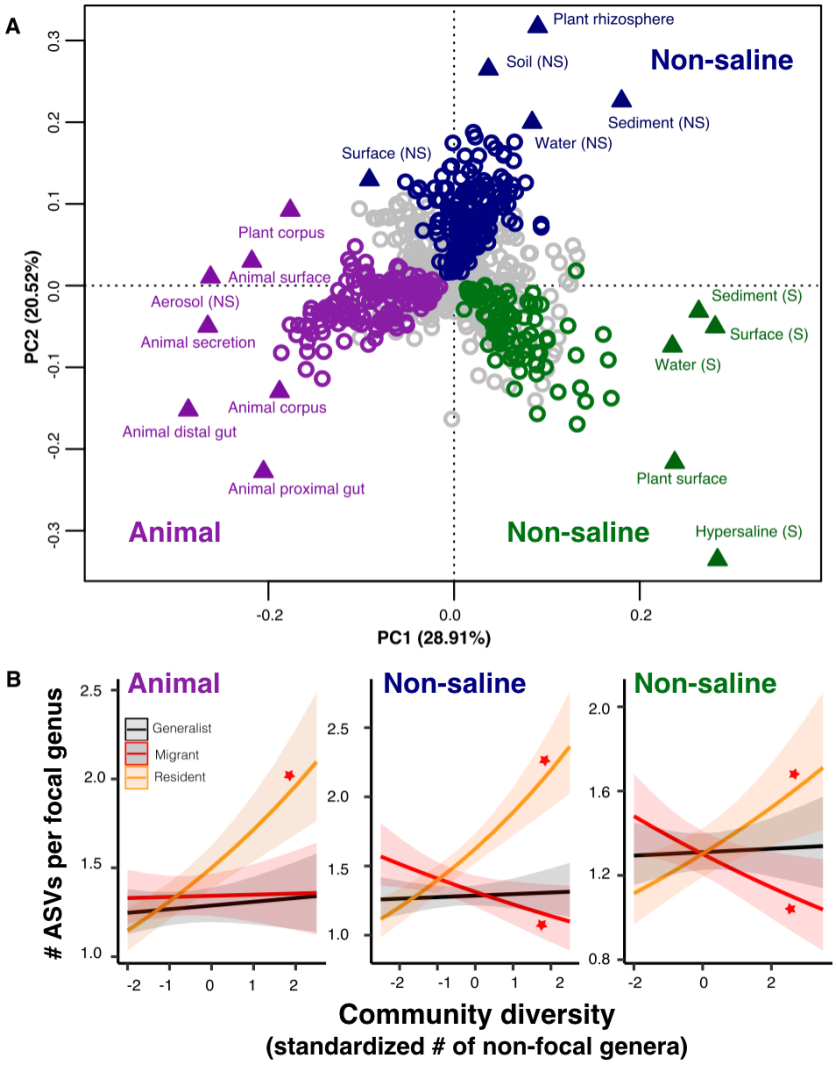

321

322 **Fig. 4. The DBD relationship varies between resident and non-resident genera. (A)**
323 **Ordination showing genera clustering into their preferred environment clusters**. The
324 matrix of 1128 genera (rows) by 17 environments (columns), with the matrix entries
325 indicating the percentage of samples from a given environment in which each genus is
326 present, was subjected to principal components analysis (PCA). Circles indicate genera
327 and triangles indicate environments (EMPO 3 biomes). Colored circles are genera
328 inferred by indicator species analysis to be residents of a certain environmental cluster,
329 and grey circles are generalist genera. The three environment clusters identified by fuzzy
330 *k*-means clustering are: Non-saline (NS, blue), saline (S, green) and animal-associated
331 (purple). Triangles of the same color indicate EMPO 3 biomes clustered into the same
332 environmental cluster. **(B) DBD in resident versus non-resident genera across**
333 **environment clusters.** Results of GLMMs modeling focal lineage diversity as a function
334 of the interaction between community diversity and resident/migrant/generalist status.
335 The x-axis shows the standardized number of non-focal resident genera (community
336 diversity); the y-axis shows the number of ASVs per focal genus. Resident focal genera
337 are shown in orange, migrant focal genera in red, and generalist focal genera in black.
338 Red stars indicate a significantly positive or negative slope (Wald test, $P<0.005$). See
339 **Supplementary Data file 2** for model goodness of fit.
340

341 **Discussion**

342 Using ~10 million individual marker sequences from the EMP, we demonstrate an overall
343 trend for diversity in focal lineages to be positively associated with overall community
344 diversity, albeit with significant variation across lineages and environments. The strength
345 of the DBD relationship dissipates with increasing microbiome diversity, which we
346 hypothesize is caused by niche saturation. In more diverse biomes such as soil, abiotic
347 factors therefore may become relatively more important in driving focal-lineage diversity.
348 The effect of DBD is strongest among habitat specialists (residents), suggesting that long-
349 term niche adaptation tends to select against the establishment of migrant diversity.

350 While most of the DBD literature considers a model of evolutionary
351 diversification (Schluter & Pennell, 2017; Whittaker, 1972), our results pertain mainly to
352 ecological community assembly dynamics. At the limited resolution of 16S rRNA gene
353 sequences, we do not expect measurable diversification within an individual microbiome
354 sample (Kuo & Ochman, 2009b); however, community diversity could still select for (as
355 in DBD) or against (as in EC) increasing diversity in a focal lineage, even if this lineage
356 diversified before the sampled community assembled. Future work with higher resolution
357 genomic or metagenomic data will enable testing if and how DBD arises in microbial
358 communities via evolutionary diversification, and also how prokaryote diversification is
359 affected by other community members including phages (Brockhurst et al., 2005),
360 protists (Meyer & Kassen, 2007), and fungi (Kastman et al., 2016). Predator-prey, cross-
361 feeding, and other biotic interactions with these non-prokaryotic community members
362 could explain some of the unaccounted variation we observed in diversity slopes across
363 environments.

364 Our dataset also provides an opportunity to explore how DBD relates with
365 genome size evolution. Bacteria with larger repertoires of accessory genes, and thus
366 larger genomes, are able to occupy a wider range of niches (Barberán et al., 2014). Taxa
367 with larger genomes might therefore be hypothesized to better survive and thrive when
368 they disperse into a new location, exhibiting stronger DBD. Although a comprehensive
369 test of this hypothesis will require higher resolution genomic or metagenomic data, as a
370 preliminary exploration we assigned genome sizes to 576 focal genera for which at least
371 one whole genome sequence was available (using the largest recorded genome size for
372 each genus) and added an interaction term between genome size and diversity as a fixed

373 effect in the GLMM (**Methods**). Consistent with our expectation, we observed a
374 significant positive effect of genome size on the diversity slope (GLMM, Wald test,
375 z=2.5, *P*=0.01; **Fig. 5, Supplementary Data file 1 Section 6**). This effect was not
376 observed in null models, in which the interaction between community diversity and focal
377 genus genome size was never significant (**Supplementary Data file 3 Section 1.3 and**
378 **2.2**) and so this effect of genome size cannot be trivially explained by data structure. The
379 positive relationship between genome size and DBD is likely even stronger than
380 estimated, because assigning genome sizes to entire genera is imprecise (*i.e.* there is
381 variation in genome size within a genus, or even within species), therefore weakening the
382 correlation.

383 The positive correlation between genome size and DBD observed here could be
384 driven by larger metabolic repertoires encoded by larger genomes (40), potentially
385 creating more opportunities to benefit from cross-feeding, niche construction (San Roman
386 & Wagner, 2018), and other interspecies interactions. This tendency appears to be at odds
387 with the Black Queen hypothesis, which predicts that social conflict between interacting
388 species leads to the inactivation and loss of genes involved in shareable metabolites
389 (public goods), eventually resulting in reduced genome size (Morris & Lenski, 2012).
390 Such a process would produce a negative correlation between the degree of species
391 interactions (*i.e.* community diversity) and genome size (Morris & Lenski, 2012). The
392 interaction between genome size, biotic interactions and diversification thus deserves
393 further study.

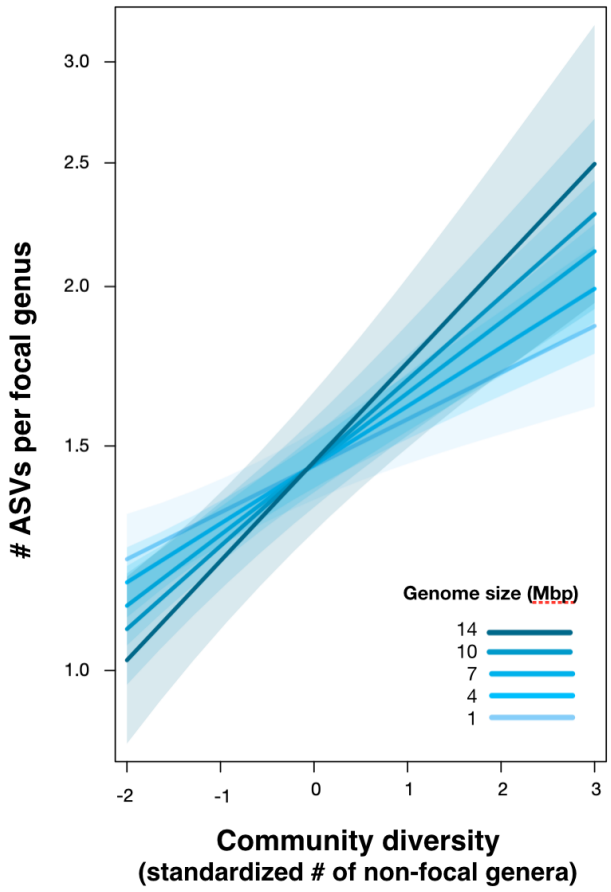

Fig. 5. Positive effect of genome size on DBD. Results are shown from a GLMM predicting focal lineage diversity as a function of the interaction between community diversity and genome size at the ASV:Genus ratio (**Supplementary Data file 1 Section 6**). The x-axis shows the standardized number of non-focal genera (community diversity); the y-axis shows the number of ASVs per focal genus. Variable diversity slopes corresponding to different genome sizes are shown in a blue color gradient; the shaded area depicts 95% confidence limits of the fitted values. See **Supplementary Data file 2** for model goodness of fit.

Alongside theory and experimental data, the EMP survey data provide a window into the biotic drivers of microbial diversity in nature. In particular, our correlational results support previous experimental and theoretical results showing that DBD is strong

407 when community diversity is low (Calcagno et al., 2017; Jousset et al., 2016), driving the
408 accumulation of diversity in a positive feedback loop until niches are filled and EC starts
409 to predominate (Bailey et al., 2013; Brockhurst et al., 2007; Gómez & Buckling, 2013;
410 Meyer & Kassen, 2007). However, due to the correlational nature of the EMP data, it is
411 not possible to test whether DBD is primarily due to the creation of novel niches via
412 biotic interactions and niche construction (Laland et al., 1999), or due to increased
413 competition leading to specialization on underexploited resources (Hibbing et al., 2010;
414 Jousset et al., 2016). We hope future higher resolution genomic studies, and
415 complementary experiments, will be able to elucidate the types of biotic interactions that
416 promote microbiome diversity. Regardless of the underlying mechanisms, our results
417 demonstrate a general scaling between different levels of community diversity, which has
418 important implications for modeling and predicting community function and stability in
419 response to perturbations (Coyte et al., 2015; Pennekamp et al., 2018). The answer to the
420 question 'why are microbiomes so diverse?' might in a large part be because
421 microbiomes are so diverse (Emerson & Kolm, 2005).
422

423 **Acknowledgements.**
424 We thank Luke Thompson for assistance obtaining EMP data and Zofia Ecaterina
425 Taranu, Vincent Fugère and Guillaume Larocque for advice on GLMMs. We are also
426 grateful to Steven Kembel, Tom Battin, the reviewers Eric Kemen and Benjamin E.
427 Wolfe, and the editor Detlef Weigel for critical comments that improved the manuscript.
428 **Funding:** This project was made possible by an NSERC Discovery Grant and Canada
429 Research Chair to BJS.

Competing interests: none to declare.

Data and materials availability: All data is available from the Earth Microbiome Project (ftp.microbio.me), as detailed in the Methods. All computer code used for analysis are available at https://github.com/Naima16/dbd.git.

Tables

Table 1. Effects of community diversity on focal lineage diversity across taxonomic ratios. The GLMMs showed statistically a significant positive effect of community diversity on focal lineage diversity. Each row reports the effect of community diversity on focal lineage diversity (Div), as well as its standard error, Wald z-statistic for its effect size and the corresponding *P*-value (left section), or standard deviation on the slope for the significant random effects (right section). SE=standard error, Env=environment type, Lin=lineage type, Lab=Principal Investigator ID, Sample=EMP Sample ID. Interactions are denoted as '*'. n.s.=not significant (likelihood-ratio test). All models provide a significantly better fit than null models without fixed effects ($\Delta AIC > 10$ and $P < 0.05$; **Supplementary Data file 2**).

	Slope (fixed effects)				**Standard deviation on the slope (random effects)**				
	Div	**SE**	**z**	***P***	**Env**	**Lin**	**Lin*Env**	**Env*Lab**	**Sample**
ASV:Genus	0.091	0.016	5.792	6.95e-09	n.s.	0.074	0.142	0.114	0.067
Genus:Family	0.047	0.008	5.911	3.41e-09	n.s.	0.071	0.07	0.039	n.s.
Family:Order	0.119	0.017	7.001	2.54e-12	0.023	0.094	0.092	0.106	n.s.
Order:Class	0.109	0.020	5.447	5.13e-08	0.05	0.141	0.078	0.051	n.s.
Class:Phylum	0.272	0.043	6.341	2.29e-10	0.119	0.174	0.119	0.114	n.s.

Table 2. GLMMs applied to data simulated under null models. Null models 1 and 2 were generated under the ZSM distribution, with a single distribution for the whole dataset (Model 1) or one distribution per environment (Model 2). Model 3 is similar to Model 1, except with a single Poisson distribution for the whole dataset, and +DBD or +EC refer to adding these effects to 100% of ASVs (see **Methods** and **Figure 2 supplement 7**). Each row reports the effect of community diversity on focal lineage diversity (Div), as well as its standard error, Wald z-statistic for its effect size and the corresponding *P*-value (Wald test) (left section), or standard deviation on the slope for the significant random effects (right section). SE=standard error, Env=environment type, Lin=lineage type, Sample=EMP Sample ID. n.s.=not significant (likelihood-ratio test), n.t.= not tested, because separate environments were not included in Models 1 or 3.

	Slope (fixed effects)				**Stand dev on the slope (random effects)**			
	Div	**SE**	**z**	***P***	**Env**	**Lin**	**Lin*Env**	**Sample**
Model 1	**-0.005**	0.000	-9.807	**<2e -16**	n.t.	0.639	n.t.	n.s.
Model 2	n.s.							
Model 3	**-0.012**	0.002	-6.552	**5.69e-11**	n.t.	0.021	n.t.	n.s.
Model 3 + DBD	**0.016**	0.001	11.48	**<2e-16**	n.t.	0.008	n.t.	n.s.
Model 3 + EC	**-0.011**	0.002	-6.14	**8.26e-10**	n.t.	ns	n.t.	n.s.

463 **Table 3. GLMMs with community diversity measured using Shannon diversity.**
464 Results are shown from GLMMs with Shannon diversity of non-focal taxa (Div) as a
465 predictor of ASVs richness of focal taxa. Each row reports the estimate (Div), as well as
466 its standard error, Wald z-statistic for its effect size and the corresponding *P*-value (Wald
467 test) (left section), or standard deviation on the slope for the significant random effects
468 (right section). SE=standard error, Env=environment type, Lin=lineage type,
469 Lab=Principal Investigator ID, Sample=EMP Sample ID. n.s.=not significant (likelihood-
470 ratio test).
471

	Fixed effects				**Random effects**				
	Div	**SE**	**z**	***P***	**Env**	**Lin**	**Env*Lin**	**Env*Lab**	**Sample**
Genus	0.055	0.013	4.33	1.49e-05	n.s.	0.08	0.15	0.085	0.054
Family	0.148	0227	6.491	8.51e-11	n.s.	0.184	0.268	0.16	0.134
Order	0.378	0.038	9.864	<2e-16	n.s.	0.34	0.417	0.258	0.202
Class	0.398	0.05	7.973	1.54e-15	n.s.	0.369	0.46	0.326	0.262
Phylum	0.319	0.088	3.614	0.0003	0.169	0.316	0.5	0.495	0.378

472

Table 4. Community diversity has a stronger effect than abiotic factors on focal lineage diversity (EMP dataset). Results are shown from GLMMs with community diversity, four abiotic factors (temperature, elevation, pH, and latitude), and their interactions with community diversity, as predictors of focal lineage diversity. Random effects on the intercept included environment, lineage, lab ID and sample ID. Each row reports the taxonomic ratio, the predictors used in the GLMM (fixed effects only), their estimate (Est), standard error (SE) and *P*-value (P) (Wald test). Interactions are denoted as '*'. Random effects are not shown.

	Predictor	Est	SE	P
ASV:Genus	**Div**	0.128	0.013	< 2e-16
	Temperature	0.04	0.014	0.00479
	Div*Temperature	0.043	0.014	0.00175
	Div*Latitude	0.031	0.013	0.02119
	Div*Elevation	-0.031	0.014	0.02829
Genus:Family	**Div**	0.094	0.009	< 2e-16
	Temperature	0.026	0.009	0.00268
	pH	-0.042	0.009	5.88e-06
Family:Order	**Div**	0.131	0.01	< 2e-16
Order:Class	**Div**	0.184	0.01	< 2e-16
	Div*Temperature	0.032	0.009	0.000827
	Div*Latitude	0.023	0.008	0.005403
Class:Phylum	**Div**	0.236	0.011	< 2e-16
	Div*Temperature	0.059	0.014	2.15e-05
	Div*Latitude	0.03	0.011	0.00884

Table 5. GLMMs applied to a soil dataset. Each row reports the taxonomic ratio, the predictors used in the GLMM (fixed effects only), their estimate (Est), standard error (SE) and *P*-value (P) (Wald test). Left columns: GLMM with community diversity (Div) and all abiotic variables considered separately, as predictors of focal lineage diversity. Right columns: GLMM with community diversity (Div) and the three first principle components (PCs) representing abiotic variables, as predictors of focal lineage diversity. n.s., non-significant (LRT test). All models provide a significantly better fit than null models without fixed effects (ΔAIC > 10 and $P < 0.05$; **Supplementary Data file 2**), except for the GLMM with abiotic factors at the Family:Order level, where latitude has a significant effect on focal lineage diversity but its effect is nearly null, with a ΔAIC between full and null model of 4 and a null marginal R^2.

	GLMMs with abiotic variables				GLMMs with the 3 first PCs			
	Predictor	**Est**	**SE**	**P**	**Predictor**	**Est**	**SE**	**P**
ASV:Genus	**Div**	n.s.			**Div**	0.064	0.016	9.47e-05
	Latitude	0.294	0.025	< 2e-16	**PC1**	-0.065	0.007	< 2e-16
	UV_light	-0.177	0.016	< 2e-16	**PC2**	-0.03	0.006	1.98e-05
	MDR	0.028	0.006	7.12e-06				
	NPP2003_2015	-0.066	0.005	< 2e-16				
	Latitude^2	-0.3	0.029	< 2e-16				
	Clay_silt^2	-0.012	0.004	0.003				
	Soil_N^2	-0.007	0.001	1.66e-06				
	Soil_C_N_ratio	0.003	0.001	0.004				
	PSEA^2	0.01	0.002	4.84e-06				
	MDR^2	0.017	0.003	2.40e-08				
	NPP2003_2015	-0.016	0.004	0.0001				
Genus:Family	**Div**	0.032	0.01	0.0011	**Div**	0.033	0.01	0.001
	Latitude	-0.035	0.006	2.04e-09	**PC1**	-0.016	0.006	0.02
					PC2	0.02	0.006	0.00089
Family:Order	**Div**	n.s.			**Div**	n.s.		
	Latitude	-0.0005	0.0002	0.0105	**PC1**	-0.026	0.007	0.00032
					Div*PC1	0.04	0.006	2.14e-12
					Div*PC3	0.023	0.005	1.68e-06
Order:Class	Null model with no predictor was significant							
Class:Phylum	**Div**	0.032	0.01	0.00174	**Div**	0.032	0.01	0.003
	pH	0.074	0.01	4.37e-13	**PC1**	-0.051	0.01	3.54e-07
					PC2	-0.028	0.01	0.006

498 **Supplementary Figure Legends**
499
500 **Figure 2 supplement 1. Distributions of diversity slope estimates across different**
501 **random effects, from the GLMMs predicting focal lineage diversity as a function of**
502 **community diversity. (A)** Class:Phylum, **(B)** Order:Class, **(C)** Family:Order, **(D)**
503 Genus:Family, and **(E)** ASV:Genus. Estimation of random effect coefficients from the
504 GLMMs (Table S1), shows that the effect of diversity on focal lineage diversity (slope
505 estimates) are generally positive but could be negative in some lineages or combinations
506 of environment, lineage (Environment*Lineage), and the laboratory that submitted the
507 dataset (Environment*Lab).
508
509 **Figure 2 supplement 2. Focal lineage diversity as a function of community diversity**
510 **across biomes in the three most prevalent phyla.** (A) Proteobacteria, (B) Bacteroidetes,
511 (C) Actinobacteria. Linear models are shown for the number of classes per phylum (y-
512 axis) as a function of community diversity (number of non-focal phyla, x-axis) in each of
513 the 17 environments (EMPO3 biomes). Only environments containing the focal lineage
514 are shown. *P*-values are Bonferroni corrected for 17 tests. Significant ($P < 0.05$) models
515 are shown with red trend lines, non-significant ($P > 0.05$) trends are shown in blue.
516
517 **Figure 2 supplement 3. Focal lineage diversity as a function of community diversity**
518 **across biomes in the three most prevalent classes.** Linear models are shown for the
519 number of orders per class (y-axis) as a function of community diversity (non-focal
520 classes, x-axis) in each of the 17 environments (EMPO3 biomes). Only environments
521 containing the focal lineage are shown. Significant positive diversity slopes are shown in
522 red, negative in blue (linear models, $P < 0.05$, Bonferroni corrected for 17 tests), and non-
523 significant in grey.
524
525 **Figure 2 supplement 4. Focal lineage diversity as a function of community diversity**
526 **across biomes in the three most prevalent orders.** Linear models are shown for the
527 number of families per order (y-axis) as a function of community diversity (non-focal
528 orders, x-axis) in each of the 17 environments (EMPO3 biomes). Only environments
529 containing the focal lineage are shown. Significant positive diversity slopes are shown in
530 red, negative in blue (linear models, $P < 0.05$, Bonferroni corrected for 17 tests), and non-
531 significant in grey.
532
533 **Figure 2 supplement 5. Focal lineage diversity as a function of community diversity**
534 **across biomes in the three most prevalent families.** Linear models are shown for
535 genera per family (y-axis) as a function of community diversity (non-focal families, x-
536 axis) in each of the 17 environments (EMPO3 biomes). Only environments containing the
537 focal lineage are shown. Significant positive diversity slopes are shown in red, negative
538 in blue (linear models, $P < 0.05$, Bonferroni corrected for 17 tests), and non-significant in
539 grey.
540
541 **Figure 2 supplement 6. Focal lineage diversity as a function of community diversity**
542 **across biomes in the three most prevalent genera.** Linear models are shown for ASVs
543 per genus (y-axis) as a function of community diversity (non-focal genera, x-axis) in each

of the 17 environments (EMPO3 biomes). Only environments containing the focal lineage are shown. Significant positive diversity slopes are shown in red, negative in blue (linear models, $P < 0.05$, Bonferroni corrected for 17 tests), and non-significant in grey.

Figure 2 supplement 7. Null models based on Neutral Theory. Results are shown from data simulated under (A) neutral Model 1, (B) neutral Model 2, or (C) neutral Model 3. Model 1 is sampled from the zero-sum multinomial distribution with a single distribution for the whole dataset, while Model 2 includes a separate distribution for each of the 17 different environments (EMPO 3 biomes). In Model 3 (C), the effect of DBD (top rows) or EC (bottom rows) are "spiked in" at different levels, ranging from 0 to 100% of ASVs in a sample. Blue lines show a linear fit, with slopes (m) estimated by GLMM in selected panels. See Methods for model details, and Table 2 and Supplementary Data file 3, Section 1.2 for full GLMM results.

Figure 2 supplement 8. Lineage diversity (mean ASV:Genus ratio among all lineages) as a function of community diversity (number of genera) in the EMP data. Samples from different environments (EMPO level 3) are shown in different colors, each with their corresponding linear model fit.

Figure 2 supplement 9. Taxonomic ratios estimated from simulated rarefied sequence data. Each panel simulates a set of microbiome samples that differ in their diversity (number of genera in left panels **A** and **B**, number of phyla in right panels **C** and **D**) while maintaining a set true taxonomic ratio (horizontal black line). **(A)** True ratio set to 2 ASVs/genus, close to the per-sample mean and median in the real EMP data, in a range of samples between 1 and 1128 named genera, as observed in the real EMP data. **(B)** True ratio set to 20 ASVs/genus, equal to the overall mean of 22,014 named ASVs in 1128 named genera, and close to the maximum ratios observed in individual samples (Fig. 2 supplement 6). Insets show the ranges of 1-50 and 51-150 genera, approximating observations from lower- or higher-diversity samples such as gut and soil, respectively (Fig. 2 supplement 6). The insets only show the rarefaction to 5,000 sequences, as used in the real EMP dataset. **(C)** True ratio set to 3 classes/phylum, close to the per-sample mean and median in the real EMP data, in a range of samples between 1 and 84 named phyla, as observed in the real EMP data. **(D)** True ratio set to 10 classes/phylum, close to the maximum ratios observed in individual samples (Fig. S2). Different rarefaction levels are shown as different colored lines.

Figure 2 supplement 10. Linear, quadratic and cubic models for the relationship between focal lineage diversity and community diversity for varying levels of % nucleotide identity. Community diversity was estimated as the number of clusters at a focal level (d_i) and focal lineage diversity as the mean of the clusters at the rank above (d_{i+1}/d_i). All P-values are < 0.001. Linear fit (grey); quadratic fit (blue), cubic fit (red); same colors for the associated adjusted R^2. The x-axis (diversity) shows the number of clusters at the focal percent-identity level (d_i), and the y-axis (diversification) is the mean of the clusters at the rank above (d_{i+1}/d_i).

Figure 2 supplement 11. Linear, quadratic and cubic models for each environment type for varying levels of % nucleotide identity. Community diversity was estimated as the number of clusters at a focal level (d_i) and focal lineage diversity as the mean of the clusters at the rank above (d_{i+1}/d_i). Linear (grey), quadratic (blue) and cubic (red), with corresponding adjusted R-squared values in the same colour. *P*-values are Bonferroni corrected for 17 tests. Significant, $P < 0.05$ (solid lines), non-significant (dashed lines). The x-axis shows the number of clusters at the focal percent-identity level (d_i), and the y-axis is the mean of the clusters at the rank above (d_{i+1}/d_i).

Figure 4 supplement 1. Resident genera of environment clusters. Results from indicator species analysis illustrated as a heatmap**.** Only the 25 resident genera with the highest indval indices and $P<0.05$ (permutation test) are shown for every environment cluster (animal-associated, non-saline and saline free). For the full results see **Supplementary Data file 5.**

Supplementary File legends

File 1. Full GLMM outputs for the EMP data.

File 2. Goodness of fit for the GLMMs.

File 3. Full GLMM output for simulated data under Neutral Theory models

File 4. Full GLMM output for soil data (Delgado et al.)

File 5. Indicator species analysis. The table shows the assignment of each genus to one of three environment types.

File 6. Genome size assignment. The table shows genome sizes assigned to each genus.

621 **Materials and Methods**

622 **Earth Microbiome Project dataset.** We used the EMP '2000 subset' of 16S rRNA gene
623 sequences, rarefied to 5000 sequences per sample. This subset contains 155,002 ASVs
624 from 2,000 samples with an even distribution across 17 natural environments (EMP
625 Ontology level 3). Data were downloaded from the EMP FTP server (ftp.microbio.me),
626 on February 9, 2018.

627

628 Specifically, 16S rRNA-V4 region reads (90 bp, GreenGenes 13.8 taxonomy) along with
629 environmental data and EMPO3 designations
630 (http://press.igsb.anl.gov/earthmicrobiome/protocols-and-standards/empo/) were
631 downloaded from the EMP FTP server (ftp.microbio.me), on February 9, 2018. Sequence
632 summaries were downloaded from :
633 ftp://ftp.microbio.me/emp/release1/otu_distributions/otu_summary.emp_deblur_90bp.sub
634 set_2k.rare_5000.tsv, environmental data from:
635 ftp://ftp.microbio.me/emp/release1/mapping_files/emp_qiime_mapping_release1.tsv, and
636 EMPO3 designations from :
637 ftp://ftp.microbio.me/emp/release1/mapping_files/emp_qiime_mapping_subset_2k.tsv.
638 The list of the associated 97 studies and 61 corresponding principal investigator identities
639 were downloaded from https://www.nature.com/articles/nature24621#s1.
640 Based on the ASV annotations across samples, we estimated the taxonomic ratio for each
641 focal lineage (ASV:Genus, Genus:Family, Family:Order, Order:Class and Class:Phylum),
642 along with the number of non-focal lineages (dbd_analys_input.py,

643 glmm_analys_input.py, Python Version 2.7). Unclassified ASVs were removed from the
644 analyses.
645
646 **Generalized linear mixed model (GLMM) analyses.** We used GLMMs to determine
647 how focal lineage diversity (*e.g.* its ASV:Genus ratio) is affected by community diversity
648 (*e.g.* non-focal genera). The effects of environment (as defined by the EMP Ontology
649 'level 3 biomes') and the focal lineage identity were included as random effects on the
650 slope and intercept. We also controlled for the submitting laboratory (identified by the
651 principal investigator) and the EMP unique sample identifier (i.e. if two taxa were part of
652 the same sample).
653 All models were fitted in Rstudio (Version 1.1.442, R Version 3.5.2) using the
654 glmer function of the lme4 package (Bates et al., 2015). Data standardization
655 (transformation to a mean of zero and a standard deviation of one) was applied to all
656 predictors to get comparable estimates. In models with only one predictor, applying
657 standardization resolved convergence warnings and considerably sped up the
658 optimization. We first tested the significance of random effects, by using likelihood-ratio
659 tests (LRTs, implemented in the anova function in the R stats package) on nested models
660 where each random effect was dropped one at a time. We then assessed the significance
661 of fixed effects using drop1 function from stats package with the likelihood-ratio test
662 option (this function drops individual terms from the full model and compares models
663 based on the AIC). We calculated the Akaike information criterion (AIC) of each
664 significant model and a null model including all random effects but no fixed effects other
665 than the intercept. We then report the difference in AIC between the full and null models

666 (ΔAIC), along with a likelihood ratio test *p*-value to assess the significance of the full
667 model relative to the null. Only significant models ($P<0.05$) are reported.
668 As an additional test of the goodness of fit for the significant models, we
669 estimated the coefficient of determination (R^2) using the r.squaredGLMM function from
670 the MuMIn R package. This function implements a method developed by Nakagawa and
671 Schielzeth and its extension for random slopes (Johnson, 2014; Nakagawa & Schielzeth,
672 2013). Two values were estimated: the marginal R^2, as a measure of the variance
673 explained only by fixed effects, and the conditional R^2 as a measure of the variance
674 explained by the entire model (both fixed effects and random effects). Only results from
675 R^2 estimation based on lognormal and trigamma methods were reported because they are
676 specific to the logarithmic link function used in all GLMMs.
677 Diagnostic plots (plot and qqnorm R functions in base and stats packages) were
678 checked for each model to ensure that residual homoscedasticity (homogeneity of
679 variance) was fulfilled: no increase of the variance with fitted values and residuals were
680 symmetrically distributed tending to cluster around the 0 of the ordinate, but with an
681 expected pattern due to count data. Normality plots were imperfect, but they generally
682 showed that the residuals were close to being normally distributed. The assumption of
683 normality is often difficult to fulfill with high numbers of observations, as is the case in
684 our models (https://www.statisticshowto.datasciencecentral.com/shapiro-wilk-test/), and
685 non-normality is less of concern than heteroscedastic for the validity of GLMMs
686 (https://bbolker.github.io/mixedmodels-misc/ecostats_chap.html#diagnostics).
687 We tested for overdispersion using the overdisp_fun R function available at
688 https://bbolker.github.io/mixedmodels-misc/glmmFAQ.html, and found that all the

689 models were not overdispersed, but rather were underdispersed : the ratio of the sum of
690 squared Pearson residuals to residual degrees of freedom was < 1 and non-significant
691 when tested with a chi-squared test. The only exception was Shannon diversity-based
692 GLMMs. In case of underdispersion and given that underdispersion leads to more
693 conservative results, we retained the GLMMs with Poisson error distribution, despite the
694 underdispersion. (GLMM FAQ; Ben Bolker and others; 25 September 2018;
695 https://bbolker.github.io/mixedmodels-misc/glmmFAQ.html#underdispersion). For
696 Shannon diversity-based GLMMs, we accounted for overdispersion by adding an
697 observation-level random effect to the GLMMs (Elston et al., 2001).
698
699 **Taxonomy-based GLMMs**
700 To test how focal lineage diversity (*e.g.* its ASV:Genus ratio) is affected by community
701 diversity (*e.g.* non-focal genera richness), for different environment types and lineages
702 across all taxonomic ratios, we used generalized linear mixed models (GLMMs) fitted on
703 the EMP dataset. As the dependent variable (focal lineage diversity, defined as taxonomic
704 ratios, ASV:Genus, Genus:Family, Family:Order, Order:Class, and Class:Phylum) was a
705 count response, we used a Poisson error distribution with a log link function. Community
706 diversity (number of non-focal lineages: non-focal Genera, Families, Orders, Classes, and
707 Phyla), standardized to a mean of zero and a standard deviation of one, was specified as
708 the predictor (fixed effect). We included the following random effects on the slope and
709 intercept: lineage (Lin), environment (Env), environment nested within lineage (a lineage
710 may be present in different environments) and lab (the principal investigator who
711 conducted the EMP study) nested within environment (different labs sampled and

712 sequenced a given environment) (as suggested in http://bbolker.github.io/mixedmodels-
713 misc/glmmFAQ.html). Defining random effects on the slope enabled us to test slope
714 variation across groups of each categorical variable (*e.g.* slope variation between different
715 environments or different lineages). We included the EMP unique sample ID as a random
716 effect to control for dependencies between observations (if two taxa were part of the
717 same sample) (**Table 1**, **Supplementary file 1 section 1)**.
718
719 **Shannon diversity-based GLMMs**
720 We also tested whether ASV diversity in a focal taxon is dependent on the diversity of all
721 other ASVs in that sample (rather than the diversity at only the focal taxonomic level, as
722 in the taxonomy-based GLMMs above). We used the Shannon diversity index, which is
723 robust to differences in sampling effort, and generally reaches a plateau at 5,000
724 sequences or fewer (48, 49). To do so, we fitted a GLMM with the number of ASVs per
725 focal taxon as the response variable, and the Shannon diversity based on ASVs across all
726 non-focal taxa (z-standardized) as the predictor (fixed effect), the random effects were
727 kept as in the taxonomy-based GLMMs, but we added an observation-level random effect
728 to account for overdispersion (**Table 3**, **Supplementary file 1 section 2**). To avoid
729 dependence between the response and predictor variables, we used the rarefied ASV
730 dataset (5,000 ASVs/sample as above) as the response variable, and the Shannon
731 diversity calculated on unrarefied data from the same samples as the predictor.
732
733 **Null models.** We considered three null models, all of which randomize the associations
734 between ASVs within a sample, thus breaking any true biotic interactions. These null

735 models were randomly generated matrices of the same size as the real EMP dataset, but
736 based on a distribution that arises from the Neutral Theory of Biodiversity. Neutral
737 Theory postulates that the biodiversity of a metacommunity is governed by independent
738 random population dynamics across species. The aggregate behaviour is quantified by the
739 fundamental biodiversity number θ, such that $\theta = 2\, J_M\, \upsilon$, where J_M is the size of the
740 metacommunity and v is the speciation rate. Parametrized by θ, the metacommunity zero-
741 sum multinomial distribution (mZSM) was developed to obtain random samples of size J
742 *(Alonso & McKane, 2004)*. We used this mZSM distribution (implemented with the *sads*
743 package in R; http://search.r-project.org/library/sads/html/dmzsm.html) to generate the
744 counts of the ASVs for each dataset in models 1 and 2. Model 1 assumes that the whole
745 dataset follows the same species abundance distribution (SAD), characterized by a
746 mZSM with $\theta = 50$. Model 2 assumes that each environment has its own SAD and thus
747 all the samples of a single environment are assigned the same θ but are distinct across
748 environments (θ was chosen uniformly between 1 and 100). The number of samples per
749 environment were the same as the EMP dataset. To obtain similar mean counts as the real
750 dataset, we set $J = 1000$ for both models 1 and 2, in order to vary θ from 1 to 100. These
751 values are reasonable based on previous studies that estimated these parameters from
752 microbiome data (Li & Ma, 2016). We included a down-sampling step to replicate the
753 zero-inflated nature of the real dataset (on average there were only 96 ASVs per sample
754 while there was a total of 22,014 ASVs in the entire EMP dataset). To replicate the
755 sampling effect due to rarefaction, we first created a vector of all individuals from a
756 single sample. We then selected 5000 individuals at random whose identities determined
757 which ASVs were found in that sample. These neutrally-derived random matrices, null

models 1 and 2, were plotted using the same plots (ASV:Genus vs number of genera) as the real EMP dataset and were then analyzed using GLMMs with community diversity as a predictor of focal lineage diversity (fixed effect), with lineage identity and EMP sample ID as random effects. For Model 1, the slope was significantly negative (GLMM, Wald test, z=-9.807, P<2e-16). For Model 2, the null GLMM (including the intercept only) was significant, meaning that the community diversity has no significant effect on focal lineages diversity (Likelihood-ratio test between the model with the predictor and the intercept-only model, P=0.9399).

To generate a null model for a metacommunity assembled by niche processes, null model 3 was made by sampling from a single Poisson distribution ($\lambda = 0.01$) for each element of the data matrix. We used the Poisson distribution as a sensitivity analysis compared to the ZSM, and found the two behave quite similarly (*i.e.* Model 1 and 3 produce qualitatively similar results). The probability of size zero was sufficiently large that the down-sampling step was not needed for this model. Next, DBD and EC effects were added to null model 3 according to the following procedure. An element was chosen at random in a sample and tested if it is empty or full (*i.e.* checks the presence/absence of a particular ASV). If the element is full then the DBD algorithm fills an empty element chosen at random in the same sample, while the EC algorithm empties a filled element in the same sample. This is to mimic the effect of DBD creating a niche for a new ASV, or EC removing a niche based on the existing diversity. The strength of DBD or EC effects were determined by the percent of elements tested. These data were analyzed with GLMMs to test the power of our models to detect DBD or EC (**Table 2**, Supplementary Data file 3 Section 2.1).

781 **Rarefaction simulation**

782 We constructed a simple simulation in which each microbiome sample may differ in total
783 diversity (*e.g.* in the observed range of genera) while maintaining a constant taxonomic
784 ratio (*e.g.* ASV:genus ratio = 2). To mimic rarefaction, we then sampled a set number of
785 sequencing reads from each synthetic community, assuming ASVs are sampled with
786 equal probability and plotted the observed taxonomic ratio (**Fig. 2 supplement 9**). This
787 simple simulation is implemented in permute_ASVs_synthetic.pl.

788

789 **Nucleotide sequence-based analysis.** We clustered ASVs at decreasing levels of
790 nucleotide identity, from 100% identical ASVs down to 75% identity (roughly equivalent
791 to phyla (Konstantinidis & Tiedje, 2005)). We estimated focal cluster diversity as the
792 mean number of descendants per cluster (e.g. number of 100% clusters per 97% cluster)
793 and plotted this against the total number of clusters (97% identity in this example). This
794 approach has the advantage of including sequences even if they come from unnamed
795 taxa. For each of the six nucleotide divergence ratios tested, the relationship between total
796 number of clusters and focal cluster diversity was positive (**Fig. 2 supplement 10**),
797 consistent with DBD and suggesting that the taxonomic analyses were qualitatively
798 unbiased.

799 Fasta files with all ASVs per sample were produced by a python script
800 (Construct_fasta_per_sample.py, Python Version 2.7) from the sequences summary file
801 (otu_summary.emp_deblur_90bp.subset_2k.rare_5000 from EMP ftp server). We
802 clustered sequences from each sample using USEARCH V9.2 and estimated sample
803 diversity as the total number of clusters at a given level (*e.g.* 97% identity) and focal

804 cluster diversity as the mean number of descendent clusters (*e.g.* number of 100%
805 clusters per 97% cluster). To describe the putative DBD or EC relationships, we tested
806 three models: linear, quadratic and cubic (lm function in R). Model comparisons were
807 based on the adjusted R^2 (**Figure 2 supplement 10**).

808 We note that diversity at level i (d_i) and at level i+1 (d_{i+1}/d_i) are not independent
809 in this analysis because d_{i+1} must be greater than or equal to d_i. To assess the effects of
810 this non-independence on the results, we conducted permutation tests by randomizing the
811 associations between d_i and d_{i+1}. Using 999 permutations, *P*-values were calculated based
812 on how many times we observed a correlation greater than that seen in the real data
813 (cor.test R function with kendall method). In each permutation, we recalculated the
814 significance test (Wald z) for the correlation in the randomized data, and then computed
815 the *P*-value based on how many times we observed a z value greater than that of the
816 original data. At all six levels of nucleotide identity, the real data always showed a
817 significantly stronger positive correlation when compared to permuted data ($P = 0.001$),
818 indicating that the DBD patterns was not an artefact of the dependence structure in the
819 data.

820 The effect of community diversity on focal cluster diversity was also tested across
821 different environments analyzed separately. We modelled this relationship with linear,
822 quadratic and cubic fits, and compared those models based on the adjusted R^2 (**Figure 2**
823 **supplement 11**).

824

825 **DBD variation across environments**

826 We tested the variation of focal lineage diversity slopes across different environments by
827 including EMPO 3 biome type as a fixed effect. We fitted a GLMM with the interaction
828 between community diversity and environment type as a predictor of focal lineage
829 diversity. All other random effects on intercept and slope were kept as in the previous
830 GLMMs (**Figure 3**, **Supplementary Data file 1 Section 3**). DBD variation across
831 environments was tested for Family:Order, Order:Class and Class:Phylum taxonomic
832 ratios, as diversity slope variation by environment was statistically significant
833 (likelihood-ratio test, $P<0.05$) for these ratios in the taxonomy based models (**Table 1**).
834

835 **Abiotic effects**

836 To test for the relative effect of biotic and abiotic environmental variables on focal
837 lineage diversity across different taxonomic ratios, we used a separate GLMM, with
838 Poisson error distribution and a log link function, for every ratio. We fitted the GLMM on
839 a subset (~10%) of the whole dataset, 192 samples (from water: saline (19) and non-
840 saline (44), surface: saline (42) and non-saline (19), sediment: saline (22) and non-saline
841 (31), soil (8) and plant rhizosphere (7)), for which measurements of four key abiotic
842 variables (temperature, pH, latitude and elevation) were available. As predictors of focal
843 lineage diversity (fixed effects), we included non-focal community diversity and abiotic
844 variables, as well as their interactions. All predictors were standardized to a mean of zero
845 and a standard deviation of one to obtain comparable estimates. The GLMM had the
846 same random effects as in the previous analysis, but only on the intercept for simplicity
847 (**Table 4**, **Supplementary file 1 section 4**).
848

849 **Soil dataset analysis**

850 We used the Delgado-Baquerizo et al. 2018 soil microbiome survey (237 samples from
851 18 countries) to further test the relative impacts of biotic versus abiotic drivers of
852 diversity. Raw data and abiotic measurements were downloaded from Figshare
853 (https://figshare.com/s/82a2d3f5d38ace925492; DOI: 10.6084/m9.figshare.5611321).
854 16S bioinformatic processing was performed using QIIME2 and Deblur with the same
855 protocol as in Thompson et al. 2017. Raw data 16S rRNA gene (V3-V4 region), were
856 processed by trimming the primers (341F/805R primer set) with qiime cutadapt trim-
857 paired, then merged using qiime vsearch join-pairs. Sequences were quality filtered and
858 denoised using Deblur with a trimming length of 400bp. The resulting 400-bp Deblur
859 BIOM table was filtered to keep only ASVs with at least 25 reads total over all samples
860 and rarefied to a depth of 5000. Taxonomy was assigned with a Naive Bayes classifier
861 trained on the V4-V3 region of 99% OTU Greengenes 13.8 sequences with qiime feature-
862 classifier. We obtained a final dataset of 186 samples and 24,252 ASVs which was used
863 as input for all statistical analysis as in the EMP dataset analysis. This data set included
864 14 environmental factors: aridity index (Aridity_Index), minimum and maximum
865 temperature (MINT and MAXT), precipitation seasonality (PSEA), mean diurnal
866 temperature range (MDR), ultra-violet (UV) radiation (UV_Light), net primary
867 productivity (NPP2003_2015), soil texture (Clay_silt), pH; total C (Soil_C), N (Soil_N)
868 and P (Soil_P) concentrations, C:N ratio (Soil_C_N_ratio) and Latitude.
869 We used a separate GLMM with Poisson error distribution and a log link function to test
870 for the effect of biotic (non-focal community diversity) and abiotic environmental
871 variables on focal lineage diversity (*e.g.* the ASV:Genus ratio for a focal genus), across

872 different taxonomic ratios. We defined non-focal taxa diversity and abiotic variables as
873 predictors (fixed effects) and the lineage identity as a random effect.

874 We also fitted the same model but with the first three principal components (PCs) from the
875 principal component analysis (PCA, rda function, vegan R package) of the abiotic variables
876 (a matrix of 237 samples (rows) by 14 abiotic variables (columns)), as well as the
877 interactions between diversity and each PC, and the interaction between PCs as predictors
878 (fixed effects).

879 Because of possible non-linear relationships between abiotic variables and diversity,
880 GLMMs were fitted with a linear and a quadratic term for every abiotic variable. The
881 quadratic terms were not significant, except for the ASV:genus ratio (**Table 5**; likelihood-
882 ratio test, $P < 2.2e-16$). The interaction terms were not significant except the interaction
883 between diversity and PCs at Family:Order ratio (likelihood-ratio test, $P = 2.182e-05$;
884 **Table 5**, **Supplementary file 4**).

885

886 **Defining residents, generalists, and migrants.** We defined a genus-level community
887 composition matrix as a matrix of 1128 genera (rows) by 17 environments (columns),
888 with the matrix entries indicating the percentage of samples from a given environment in
889 which each genus is present. We clustered the environmental samples based on their
890 genus-level community composition using fuzzy *k*-means clustering. The clustering
891 (cmeans function, package e1071 in R) was done on the 'hellinger' transformed data
892 (decostand function, vegan R package). To identify resident genera to each cluster, we
893 used indicator species analysis (Dufrene & Legendre, 1997) as implemented in the indval

894 function (labdsv R package). We defined residents as genera with indval indices between
895 0.4 and 0.9, with permutation test $P < 0.05$. Genera not associated with any cluster were
896 considered generalists. We used principal component analysis (PCA) on the community
897 composition matrix to visualize the clustering and the indicator genera (rda function,
898 vegan R package) (**Figure 4**). We then ran a separate GLMM for each environmental
899 cluster, with resident genus-level diversity (number of non-focal genera) as a predictor of
900 focal genus diversity (ASV:Genus ratio) for resident, migrant (residents of one cluster
901 found in a different cluster) and generalist genera. The fixed effect was specified as the
902 interaction between diversity and a factor defining the genus-cluster association (with
903 three levels: resident, migrant and generalist). Random effects on intercept and slope
904 were kept as in the GLMMs described above.
905
906 **Genome size analysis.** We chose a subset of genera represented by one or more
907 sequenced genomes in the NCBI microbial genomes database
908 (https://www.ncbi.nlm.nih.gov/genome/browse#!/prokaryotes/). For these genera, a
909 representative genome size was assigned by selecting the genome with the lowest number
910 of scaffolds (if no closed genomes were available) (**Supplementary file 6**). If multiple
911 genomes were available with the same level of completion, the largest genome size was
912 used, as smaller genomes could be artefacts of incomplete assembly which would bias the
913 mean and median downward. Moreover, given the deletional bias in bacterial genomes
914 (Kuo & Ochman, 2009a), the largest genome is likely more reflective of the ancestral
915 genome size of the genus. Only genera with two or more ASVs in at least one sample
916 were included in the analysis. Intracellular symbionts were excluded. We fitted a GLMM

917 on the subset of data with known genome size (576 genera, ranging from ~1 to 15 Mbp)
918 with the interaction between community diversity and genome size as a predictor of focal
919 lineage diversity at the ASV:Genus level. All the other random effects on intercept and
920 slope were kept as in the previous GLMMs (**Supplementary file 1 section 6)**.
921

References

Alonso, D., & McKane, A. J. (2004). Sampling Hubbell's neutral theory of biodiversity: Sampling neutral theory. *Ecology Letters*, *7*(10), 901–910. https://doi.org/10.1111/j.1461-0248.2004.00640.x

Auguet, J.-C., Barberan, A., & Casamayor, E. O. (2010). Global ecological patterns in uncultured Archaea. *The ISME Journal*, *4*(2), 182–190. https://doi.org/10.1038/ismej.2009.109

Azaele, S., Suweis, S., Grilli, J., Volkov, I., Banavar, J. R., & Maritan, A. (2016). Statistical mechanics of ecological systems: Neutral theory and beyond. *Reviews of Modern Physics*, *88*(3), 035003. https://doi.org/10.1103/RevModPhys.88.035003

Bailey, S. F., Dettman, J. R., Rainey, P. B., & Kassen, R. (2013). Competition both drives and impedes diversification in a model adaptive radiation. *Proceedings. Biological Sciences / The Royal Society*, *280*(1766), 20131253. https://doi.org/10.1098/rspb.2013.1253

Barberán, A., Ramirez, K. S., Leff, J. W., Bradford, M. a., Wall, D. H., & Fierer, N. (2014). Why are some microbes more ubiquitous than others? Predicting the habitat breadth of soil bacteria. *Ecology Letters*, *17*(7), 794–802. https://doi.org/10.1111/ele.12282

Bates, D., Mächler, M., Bolker, B., & Walker, S. (2015). Fitting Linear Mixed-Effects Models Using lme4. *Journal of Statistical Software*, *67*(1), 1–48. https://doi.org/10.18637/jss.v067.i01

Brockhurst, M. A., Buckling, A., & Rainey, P. B. (2005). The effect of a bacteriophage on diversification of the opportunistic bacterial pathogen, *Pseudomonas aeruginosa*.

Proceedings. Biological Sciences / The Royal Society, *272*(1570), 1385–1391. https://doi.org/10.1098/rspb.2005.3086

Brockhurst, M. A., Colegrave, N., Hodgson, D. J., & Buckling, A. (2007). Niche occupation limits adaptive radiation in experimental microcosms. *PloS One*, *2*(2), e193. https://doi.org/10.1371/journal.pone.0000193

Calcagno, V., Jarne, P., Loreau, M., Mouquet, N., & David, P. (2017). Diversity spurs diversification in ecological communities. *Nature Communications*, *8*, 15810. https://doi.org/10.1038/ncomms15810

Coyte, K. Z., Schluter, J., & Foster, K. R. (2015). The ecology of the microbiome: Networks, competition, and stability. *Science*, *350*(6261), 663–666. https://doi.org/10.1126/science.aad2602

Czárán, T. L., Hoekstra, R. F., & Pagie, L. (2002). Chemical warfare between microbes promotes biodiversity. *Proceedings of the National Academy of Sciences of the United States of America*, *99*(2), 786–790. https://doi.org/10.1073/pnas.012399899

Delgado-Baquerizo, M., Oliverio, A. M., Brewer, T. E., Benavent-González, A., Eldridge, D. J., Bardgett, R. D., Maestre, F. T., Singh, B. K., & Fierer, N. (2018). A global atlas of the dominant bacteria found in soil. *Science*, *359*(6373), 320–325. https://doi.org/10.1126/science.aap9516

de Wit, R., & Bouvier, T. (2006). "Everything is everywhere, but, the environment selects"; what did Baas Becking and Beijerinck really say? *Environmental Microbiology*, *8*(4), 755–758. https://doi.org/10.1111/j.1462-2920.2006.01017.x

Dufrene, M., & Legendre, P. (1997). Species Assemblages and Indicator Species: The Need for a Flexible Asymmetrical Approach. *Ecological Monographs*, *67*(3), 345–

366. https://doi.org/10.2307/2963459

Elston, D. A., Moss, R., Boulinier, T., Arrowsmith, C., & Lambin, X. (2001). Analysis of aggregation, a worked example: numbers of ticks on red grouse chicks. *Parasitology*, *122*(Pt 5), 563–569. https://doi.org/10.1017/s0031182001007740

Elton, C. (1946). Competition and the Structure of Ecological Communities. *The Journal of Animal Ecology*, *15*(1), 54–68. https://doi.org/10.2307/1625

Emerson, B. C., & Kolm, N. (2005). Species diversity can drive speciation. *Nature*, *434*(7036), 1015–1017. https://doi.org/10.1038/nature03450

Falkowski, P. G., Fenchel, T., & Delong, E. F. (2008). The microbial engines that drive Earth's biogeochemical cycles. *Science*, *320*(5879), 1034–1039. https://doi.org/10.1126/science.1153213

Gause, G. F. (2003). *The Struggle for Existence* (Williams & Wilkins, Baltimore, 1934).

Gómez, P., & Buckling, A. (2013). Real-time microbial adaptive diversification in soil. *Ecology Letters*, *16*(5), 650–655. https://doi.org/10.1111/ele.12093

Gotelli, N. J., & Colwell, R. K. (2001). Quantifying biodiversity: procedures and pitfalls in the measurement and comparison of species richness. *Ecology Letters*, *4*(4), 379–391. https://doi.org/10.1046/j.1461-0248.2001.00230.x

Gotelli, N. J., & McGill, B. J. (2006). Null Versus Neutral Models: What's The Difference? *Ecography*, *29*(5), 793–800. https://doi.org/10.1111/j.2006.0906-7590.04714.x

Harris, K., Parsons, T. L., Ijaz, U. Z., Lahti, L., Holmes, I., & Quince, C. (2017). Linking Statistical and Ecological Theory: Hubbell's Unified Neutral Theory of Biodiversity as a Hierarchical Dirichlet Process. *Proceedings of the IEEE*, *105*(3), 516–529.

https://doi.org/10.1109/JPROC.2015.2428213

Hibbing, M. E., Fuqua, C., Parsek, M. R., & Peterson, S. B. (2010). Bacterial competition: surviving and thriving in the microbial jungle. *Nature Reviews Microbiology*, *8*(1), 15–25. https://doi.org/10.1038/nrmicro2259

Hubbell, S. P. (2001). *The Unified Neutral Theory of Biodiversity and Biogeography*. Princeton University Press.

Hug, L. A., Baker, B. J., Anantharaman, K., Brown, C. T., Probst, A. J., Castelle, C. J., Butterfield, C. N., Hernsdorf, A. W., Amano, Y., Kotaro, I., Suzuki, Y., Dudek, N., Relman, D. A., Finstad, K. M., Amundson, R., Thomas, B. C., & Banfield, J. F. (2016). A new view of the tree and life's diversity. *Nature Microbiology*, 1, 16048 https://doi.org/10.1038/nmicrobiol.2016.48

Jarvinen, O. (1982). Species-To-Genus Ratios in Biogeography: A Historical Note. *Journal of Biogeography*, *9*(4), 363–370. https://doi.org/10.2307/2844723

Johnson, P. C. (2014). Extension of Nakagawa & Schielzeth's R2GLMM to random slopes models. *Methods in Ecology and Evolution / British Ecological Society*, *5*(9), 944–946. https://doi.org/10.1111/2041-210X.12225

Jousset, A., Eisenhauer, N., Merker, M., Mouquet, N., & Scheu, S. (2016). High functional diversity stimulates diversification in experimental microbial communities. *Science Advances*, *2*(6), e1600124. https://doi.org/10.1126/sciadv.1600124

Kastman, E. K., Kamelamela, N., Norville, J. W., Cosetta, C. M., Dutton, R. J., & Wolfe, B. E. (2016). Biotic Interactions Shape the Ecological Distributions of Staphylococcus Species. *mBio*, *7*(5). https://doi.org/10.1128/mBio.01157-16

Kennedy, A. C., & de Luna, L. Z. (2005). Rhizhosphere. In D. Hillel (Ed.), *Encyclopedia of Soils in the Environment* (pp. 399–406). Elsevier. https://doi.org/10.1016/B0-12-348530-4/00163-6

Konstantinidis, K. T., & Tiedje, J. M. (2005). Towards a genome-based taxonomy for prokaryotes. *Journal of Bacteriology*, *187*(18), 6258–6264.

Kuo, C.-H., & Ochman, H. (2009a). Deletional bias across the three domains of life. *Genome Biology and Evolution*, *1*, 145–152. https://doi.org/10.1093/gbe/evp016

Kuo, C.-H., & Ochman, H. (2009b). Inferring clocks when lacking rocks: the variable rates of molecular evolution in bacteria. *Biology Direct*, *4*, 35. https://doi.org/10.1186/1745-6150-4-35

Laland, K. N., Odling-Smee, F. J., & Feldman, M. W. (1999). Evolutionary consequences of niche construction and their implications for ecology. *Proceedings of the National Academy of Sciences of the United States of America*, *96*(18), 10242–10247. https://doi.org/10.1073/pnas.96.18.10242

Lapierre, P., & Gogarten, J. P. (2009). Estimating the size of the bacterial pan-genome. *Trends in Genetics: TIG*, *25*(3), 107–110. https://doi.org/10.1016/j.tig.2008.12.004

Lauber, C. L., Hamady, M., Knight, R., & Fierer, N. (2009). Soil pH as a predictor of soil bacterial community structure at the continental scale: a pyrosequencing-based assessment. *Applied and Environmental Microbiology*. 75, 5111-5120. http://aem.asm.org/content/early/2009/06/05/AEM.00335-09.short

Li, L., & Ma, Z. S. (2016). Testing the Neutral Theory of Biodiversity with Human Microbiome Datasets. *Scientific Reports*, *6*, 31448. https://doi.org/10.1038/srep31448

Lindow, S. E., & Brandl, M. T. (2003). Microbiology of the phyllosphere. *Applied and Environmental Microbiology*, *69*(4), 1875–1883. https://doi.org/10.1128/aem.69.4.1875-1883.2003

Louca, S., Mazel, F., Doebeli, M., & Parfrey, L. W. (2019). A census-based estimate of Earth's bacterial and archaeal diversity. *PLoS Biology*, *17*(2), e3000106. https://doi.org/10.1371/journal.pbio.3000106

Louca, S., & Pennell, M. W. (2020). Extant timetrees are consistent with a myriad of diversification histories. *Nature*, *580*(7804), 502–505. https://doi.org/10.1038/s41586-020-2176-1

Louca, S., Shih, P. M., Pennell, M. W., Fischer, W. W., Parfrey, L. W., & Doebeli, M. (2018). Bacterial diversification through geological time. *Nature Ecology & Evolution*, *2*(9), 1458–1467. https://doi.org/10.1038/s41559-018-0625-0

Lozupone, C. A., & Knight, R. (2007). Global patterns in bacterial diversity. *Proceedings of the National Academy of Sciences of the United States of America*, *104*(27), 11436–11440. https://doi.org/10.1073/pnas.0611525104

Marshall, C. R. (2017). Five palaeobiological laws needed to understand the evolution of the living biota. *Nature Ecology & Evolution*, *1*(6), 165. https://doi.org/10.1038/s41559-017-0165

Meyer, J. R., & Kassen, R. (2007). The effects of competition and predation on diversification in a model adaptive radiation. *Nature*, *446*(7134), 432–435. http://www.nature.com/doifinder/10.1038/nature05599

Morris, J. J., & Lenski, R. E. (2012). The Black Queen Hypothesis: evolution of dependencies through adaptive gene loss. *mBio*. 3, e00036-12

http://mbio.asm.org/content/3/2/e00036-12.short

Nakagawa, S., & Schielzeth, H. (2013). A general and simple method for obtaining R 2 from generalized linear mixed-effects models. *Methods in Ecology and Evolution / British Ecological Society*, *4*(2), 133–142. https://doi.org/10.1111/j.2041-210x.2012.00261.x

Needham, D. M., & Fuhrman, J. A. (2016). Pronounced daily succession of phytoplankton , archaea and bacteria following a spring bloom. *Nature Microbiology*, 1, 16005. https://doi.org/10.1038/NMICROBIOL.2016.5

Palmer, M. W., & Maurer, T. A. (1997). Does Diversity Beget Diversity? A Case Study of Crops and Weeds. *Journal of Vegetation Science*, *8*(2), 235–240. https://doi.org/10.2307/3237352

Parks, D. H., Chuvochina, M., Waite, D. W., Rinke, C., Skarshewski, A., Chaumeil, P.-A., & Hugenholtz, P. (2018). A standardized bacterial taxonomy based on genome phylogeny substantially revises the tree of life. *Nature Biotechnology*, *36*(10), 996–1004. https://doi.org/10.1038/nbt.4229

Pennekamp, F., Pontarp, M., Tabi, A., Altermatt, F., Alther, R., Choffat, Y., Fronhofer, E. A., Ganesanandamoorthy, P., Garnier, A., Griffiths, J. I., Greene, S., Horgan, K., Massie, T. M., Mächler, E., Palamara, G. M., Seymour, M., & Petchey, O. L. (2018). Biodiversity increases and decreases ecosystem stability. *Nature*, *563*(7729), 109–112. https://doi.org/10.1038/s41586-018-0627-8

Power, J. F., Carere, C. R., Lee, C. K., Wakerley, G. L. J., Evans, D. W., Button, M., White, D., Climo, M. D., Hinze, A. M., Morgan, X. C., McDonald, I. R., Cary, S. C., & Stott, M. B. (2018). Microbial biogeography of 925 geothermal springs in

New Zealand. *Nature Communications*, *9*(1), 2876. https://doi.org/10.1038/s41467-018-05020-y

Price, T. D., Hooper, D. M., Buchanan, C. D., Johansson, U. S., Tietze, D. T., Alström, P., Olsson, U., Ghosh-Harihar, M., Ishtiaq, F., Gupta, S. K., Martens, J., Harr, B., Singh, P., & Mohan, D. (2014). Niche filling slows the diversification of Himalayan songbirds. *Nature*. 509, 222-225 https://doi.org/10.1038/nature13272

Rabosky, D. L., Chang, J., Title, P. O., Cowman, P. F., Sallan, L., Friedman, M., Kaschner, K., Garilao, C., Near, T. J., Coll, M., & Alfaro, M. E. (2018). An inverse latitudinal gradient in speciation rate for marine fishes. *Nature*, *559*(7714), 392–395. https://doi.org/10.1038/s41586-018-0273-1

Rabosky, D. L., & Hurlbert, A. H. (2015). Species richness at continental scales is dominated by ecological limits. *The American Naturalist*, *185*(5), 572–583. https://doi.org/10.1086/680850

San Roman, M., & Wagner, A. (2018). An enormous potential for niche construction through bacterial cross-feeding in a homogeneous environment. *PLoS Computational Biology*, *14*(7), e1006340. https://doi.org/10.1371/journal.pcbi.1006340

Schluter, D., & Pennell, M. W. (2017). Speciation gradients and the distribution of biodiversity. *Nature*, *546*(7656), 48–55. https://doi.org/10.1038/nature22897

Sender, R., Fuchs, S., & Milo, R. (2016). Revised Estimates for the Number of Human and Bacteria Cells in the Body. *PLoS Biology*, *14*(8), e1002533. https://doi.org/10.1371/journal.pbio.1002533

Seth, E. C., & Taga, M. E. (2014). Nutrient cross-feeding in the microbial world.

Frontiers in Microbiology, *5*, 350. https://doi.org/10.3389/fmicb.2014.00350

Sogin, M. L., Morrison, H. G., Huber, J. A., Welch, D. M., Huse, S. M., Neal, P. R., Arrieta, J. M., & Herndl, G. J. (2006). Microbial diversity in the deep sea and the underexplored "rare biosphere." *Proceedings of the National Academy of Sciences of the United States of America*, *103*(32), 12115–12120.

Sriswasdi, S., Yang, C.-C., & Iwasaki, W. (2017). Generalist species drive microbial dispersion and evolution. *Nature Communications*, *8*(1), 1162. https://doi.org/10.1038/s41467-017-01265-1

Sunagawa, S., Coelho, L. P., Chaffron, S., Kultima, J. R., Labadie, K., Salazar, G., Djahanschiri, B., Zeller, G., Mende, D. R., Alberti, A., Cornejo-Castillo, F. M., Costea, P. I., Cruaud, C., d'Ovidio, F., Engelen, S., Ferrera, I., Gasol, J. M., Guidi, L., Hildebrand, F., … Bork, P. (2015). Ocean plankton. Structure and function of the global ocean microbiome. *Science*, *348*(6237), 1261359. https://doi.org/10.1126/science.1261359

Thompson, L. R., Sanders, J. G., McDonald, D., Amir, A., Ladau, J., Locey, K. J., Prill, R. J., Tripathi, A., Gibbons, S. M., Ackermann, G., Navas-Molina, J. A., Janssen, S., Kopylova, E., Vázquez-Baeza, Y., González, A., Morton, J. T., Mirarab, S., Xu, Z. Z., Jiang, L., … Zhao, H. (2017). A communal catalogue reveals Earth's multiscale microbial diversity. *Nature*, 551, 457-463. https://doi.org/10.1038/nature24621

Vos, M. (2011). A species concept for bacteria based on adaptive divergence. *Trends in Microbiology*, *19*(1), 1–7. https://doi.org/10.1016/j.tim.2010.10.003

Whitman, W. B., Coleman, D. C., & Wiebe, W. J. (1998). Prokaryotes: the unseen majority. *Proceedings of the National Academy of Sciences of the United States of*

America, *95*(12), 6578–6583. https://doi.org/10.1073/pnas.95.12.6578

Whittaker, R. H. (1972). Evolution and Measurement of Species Diversity. *Taxon*, *21*(2/3), 213–251. https://doi.org/10.2307/1218190